NATURAL GELS: CRYSTAL-CHEMISTRY OF SHORT RANGE ORDERED COMPONENTS IN Al, Fe, AND Si SYSTEMS

Philippe ILDEFONSE, *and* ***Georges CALAS***
Laboratoire de Minéralogie-Cristallographie, UA CNRS 09,
Universités Paris 6 et 7 and IPGP,
4 place Jussieu, 75252 Paris cedex 05

INTRODUCTION

At the Earth's surface, gels are a common residual weathering product and precipitate during the first steps of weathering of crystallized parent silicate minerals and glasses (Wada, 1977, Farmer and Russell, 1990). They are also found in stream and spring deposits (Childs *et al.*, 1990a, 1990b, Inoue and Yoshida, 1990), or in low temperature hydrothermal alteration systems. These metastable phases are highly reactive and poorly crystallized. Due to the lack of long ranger order (>5 Å) in these mineral components, no definite structural model exists and the determination of their structural properties requires the use of spectroscopic methods (FTIR, NMR, XAS). In this review, the most important inorganic natural gels will be presented: opal, aluminosilicates (allophanes) and hydrous iron oxides and silicates. The data obtained allow to better understand the crystal-chemistry of these natural gels and their possible transformation processes to crystalline phases.

MATERIALS

The amorphous aluminosilicates investigated encompass the range of Al/Si ratios encountered in these natural gels: Al/Si=0.12 (opal precipitated at 180°C, Uno4, Salton sea geothermal field: Manceau et al., 1995), Al/Si=1.2 (Si-rich allophane, Ok, from weathered andesitic ashes: Yoshinaga and Aomine, 1962), Al/Si=1.4 (Si-rich allophane, PC829, from Silica Spring, New Zealand: Childs et al., 1990a) and Al/Si=1.8 (Al-rich allophane, KiP, from weathered dacitic pumice: van der Gaast *et al.*, 1985). Ferric gels are represented by an hydrous Fe-Si gel precipitated at 250°C, with Fe/Si=0.72 (Uno1, Salton sea geothermal field: Manceau et al., 1995) and by Si-bearing ferric oxides from spring precipitates (Fe/Si=2.81, Pontgibaud, France), or from volcanic formations (Fe/Si= 1.80, Hamilton, New-Zealand).

STRUCTURE OF NATURAL XRD-AMORPHOUS ALUMINOSILICATES

The natural gels studied yield only very broad XRD bands (Fig 1A). The diagram of Uno4 sample is characteristic of A-opal, with a single broad band centered around 27°

2θ (3.9 Å). Al-rich allophane (KiP) yield three diffuse bands at 10, 29-30 and 46-47 ° 2θ. Si-rich allophanes are also characterized by three broad bands at 6-7, 30, and 46-47 ° 2θ, but the band centered around 30 ° 2q is more assymetric and extend from 25 to 40 ° 2θ. These differences reflect modifications in the silica framework geometry as a function of the gel composition. Additional structural information may be obtained with spectroscopic methods. FTIR spectra indicate a shift of the Si-O-Si stretching bands from 971 cm^{-1} in Al-rich allophane to 1095 cm^{-1} in A-opal, related to an increase of the polymerization of the silica framework. In opals, this peak varies from 1100 cm^{-1} in Al-free samples to 1090 cm^{-1} in the Uno4 Al-opal, suggesting the presence of 4-fold Al in the opal framework. This evidence is consistent with the chemical analysis (8.22 weight percent Al_2O_3) and the results obtained by ^{27}Al NMR (Manceau et al., 1995; see below). In Al-rich allophane, the absorption band at 348 cm^{-1} is more intense than in Si-rich allophanes, a signature of imogolite-like structural units (imogolite is a bidimensional structure with 6-coordinated Al and isolated Si-tetrahedra).

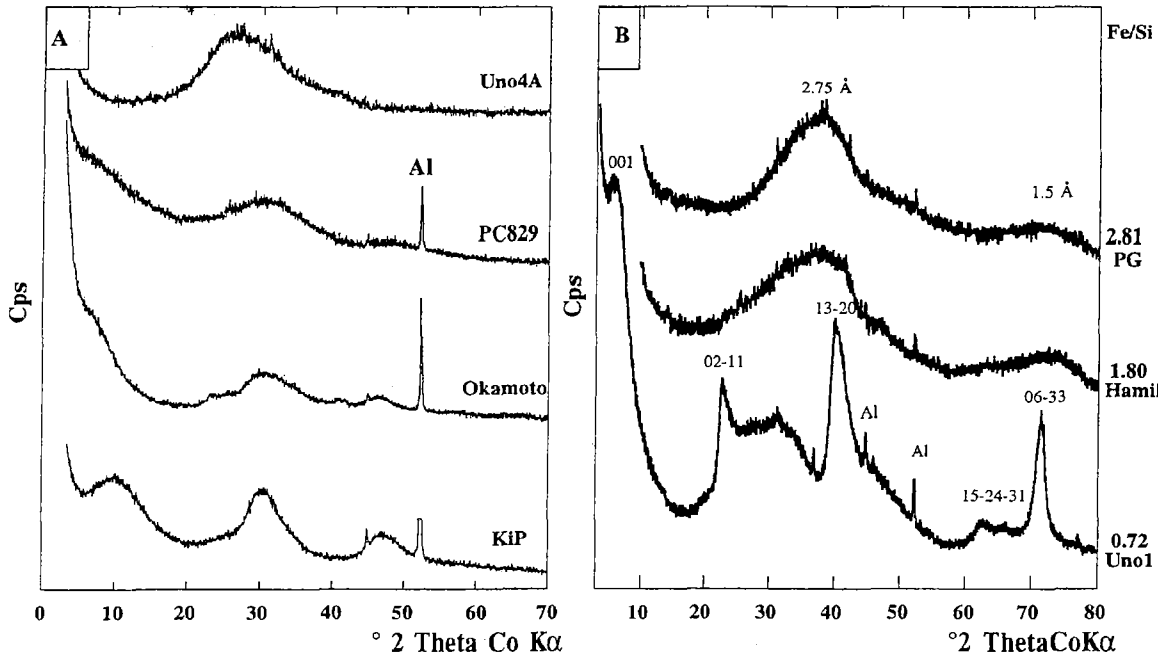

Figure 1: XRD patterns of studied aluminosilicates (A), ferric silicate and Si-iron oxides (B) (Al: sample holder)

For a better understanding of the local Al environment in these silicates, we used two element specific probes Al-K XANES, and ^{27}Al MASNMR. Al K-XANES spectra of allophanes are characterized by three main resonances, A, B and C (Figure 2A), the position of which remains at the same energy as in 6-fold Al reference compounds. The edge maximum corresponds to the B component, an indication of majority 6-fold Al sites and occurs at the same position as in 2:1 phyllosilicates which contain only one type of 6-fold Al site (e.g., smectites: Ildefonse *et al.*, 1994, 1997). The C component has a lower intensity and the intensity ratio C/B remains constant at 0.80-0.84. These XANES spectra are different from those of minerals with more than one octahedral Al site, such as gibbsite, halloysite and kaolinite. In these samples, the edge maximum corresponds to the C component (Ildefonse *et al.*, 1994).

Despite a similar overall shape, XANES spectra show significant variations of the A resonance relative intensity among the samples. In allophanes, the increase of the relative intensity of the A shoulder shows the presence of ^{IV}Al and indicates an increasing ^{IV}Al/^{total}Al ratio with decreasing Al/Si ratio. The ^{IV}Al/^{total}Al ratio derived from XANES spectroscopy is 8 % in Al-rich allophane (KiP), 18 % in Si-rich soil allophane (Okamoto) and up to 34% in Silica spring allophane (PC829). In Uno4 opal, all Al occurs in four-fold coordination as evidenced by an unique peak at 1566 eV.

The ^{27}Al MAS NMR spectrum of Uno4 opal (Figure 2B) consists of a single peak at 54 ppm related to ^{IV}Al. On the contrary, the main peak observed in allophanes studied is located at 5-6 ppm, and indicates that aluminum atoms are mainly six-coordinated (Müller *et al.*, 1981). In addition, there are small peaks at 59.6 and 58.6 ppm due to ^{IV}Al. Stream allophane (PC829) is also characterized by a third small peak at 33 ppm which may be related to ^{V}Al. Derived ^{IV}Al/^{total}Al ratios from NMR increase with decreasing Al/Si ratio. It is lowest for Al-rich allophane (0.04) and highest for Si-rich allophanes (0.26 for PC829, and 0.21 for Okamoto) in which the Al/Si ratio is close to unity.

The Okamoto allophane was selected for CPMAS NMR because it has a high ^{IV}Al/^{total}Al ratio, thus enabling an investigation of proton interaction with the two kinds of Al-sites. Both ^{VI}Al and ^{IV}Al have their maximum CP intensities at a contact time of 0.1 ms. At this contact time, the intensity of the ^{IV}Al resonance decreases relative to the MAS spectrum (Figure 2C). In these conditions, the apparent ^{IV}Al/^{total}Al ratio is 0.135, compared to 0.21 in the MAS experiment. This difference indicates that the protons more efficiently cross polarize ^{VI}Al than ^{IV}Al. The similarity of the contact times with maximum CP intensity for both ^{VI}Al and ^{IV}Al suggests the presence of ^{IV}Al-O-H linkages as well as ^{VI}Al -O-H linkages. The presence of ^{IV}Al-O-H linkages is consistent with these sites being Bronsted acid sites and with the pH-dependent surface charges of ^{IV}Al-bearing allophanes.

The ^{29}Si-MAS NMR spectra of opal and allophanes studied show significant differences in relation with their Al/Si ratios (Figure 2D). Two types of spectra may be distinguished for the allophanes studied: 1) Al-rich allophane (KiP) has a spectrum very close to that of imogolite and present a main sharp (3ppm) resonance at about -78 ppm; 2) Si-rich samples with Al:Si ratios near 1 have additional broad (20ppm) and poorly resolved resonances at higher negative δ_p values (centered at about -85 to -90 ppm), these latter features being due to more polymerized silicon species. This range of δ_p implies a variety of polymerized sites from Q^0 to Q^4 sites but also covers the entire range of chemical shifts observed for silicon in framework aluminosilicates with from 4 to 0 next-nearest neighbor Al atoms (-75 to -120 ppm). These counteracting effects of increasing polymerization and increasing tetraedral Al content make it difficult to interpret ^{29}Si δ_p in aluminosilicate gels. ^{27}Al MASS NMR indicates that ^{IV}Al increased as Al:Si ratio decreased. An inverse correlation exists between the ^{IV}Al % estimated from the ^{27}Al NMR spectra and the intensity of the -79 ppm resonance. Besides a positive correlation is indicated by the relation between the relative fraction of the resonance at about -85

ppm and the % of ^{IV}Al. These data traduce that the amounts of the more polymerized units correlate with the fraction of 4-fold Al, suggesting the presence of more polymerized and aluminous structural units in the natural allophanes.

In opal studied, the ^{29}Si-MAS NMR spectrum exhibits a large peak centered around -110 ppm with a full width at half maximum of 17.6 ppm (Figure 2D). This chemical shift corresponds to Si atoms coordinated to four oxygens in a three dimensional array of corner sharing tetrahedra. The assymetry towards less negative values indicates that the chemical environment about the Si tetrahedra is not unique. This spectrum was decomposed into three Gaussian components at -111.8, -104.7 and 98.9 ppm (Manceau et al., 1995), corresponding to Si tetrahedra bridged to 4 Si, 3 Si+1Al and 2Si+2Al, respectively (Lippmaa et al., 1980).

STRUCTURE OF NATURAL SI-BEARING FERRIC OXIDES

Two kinds of XRD patterns may be distinguished among the iron silicates studied (Figure 1B). The Uno1 pattern closely resembles those of natural hisingerite and synthetic ferric smectite. A broad basal reflection occurs near 5.7 ° 2θ (18 Å) and two-dimensional hk diffraction bands occur near 22.7 ° 2θ (4.56 Å), 40.1° 2θ (2.61 Å), 62.5° 2θ (1.7 Å) and 71.4° 2θ (1.53 Å). These features are characteristic of diffraction bands of a turbostratic layer silicate. The b axis based on 06-33 is 9.20 Å, which corresponds to hisingerite and nontronite. XRD patterns of the two other samples (Figure 1B), with lowest Fe/Si ratios, characterize 2-line ferrihydrites (Childs et al, 1990b). Nevertheless, the maximum, at 38° 2θ (2.75 Å) is displaced towards lower angles as in Si-rich ferrihydrite. The FTIR spectrum of Uno1 is close to that of nontronite, but without the OH libration bands near 800 cm^{-1}. FTIR spectra of the two other Si-Fe oxides are characracterized by Si-O stretching bands at 970 and 1002 cm^{-1}. The shift to higher wavenumbers is well correlated to Fe/Si values, and is related to an increase of polymerization of silica units.

Local Fe and Si environment have been studied by X-ray absorption spectroscopy at the Fe- and Si-K edges. Due to the high amount of paramagnetic iron in these samples, NMR cannot be performed.

In Uno 1 sample (Fe/Si=0.72), the local environment of Fe and Si is close to that found in nontronite. The most prominent difference between Uno1 and nontronite Fe-EXAFS spectra is the amplitude lowering of the former which is an indication of structural disorder. The radial distribution function yields two well resolved peaks (Figure 3A) which correspond to 6 (O,OH) at 2.00 Å, and 3 Fe at 3.08 Å (Manceau et al., 1995). This Fe-Fe distance is consistent with the b-dimension calculated by XRD and is close to that reported in nontronite (3.07 Å). Si-K EXAFS spectra of Uno1 and nontronite have very similar lineshapes, which indicates close similarities of local structures near the Si atoms. The radial distribution function yields two well resolved peaks (Figure 3B) which

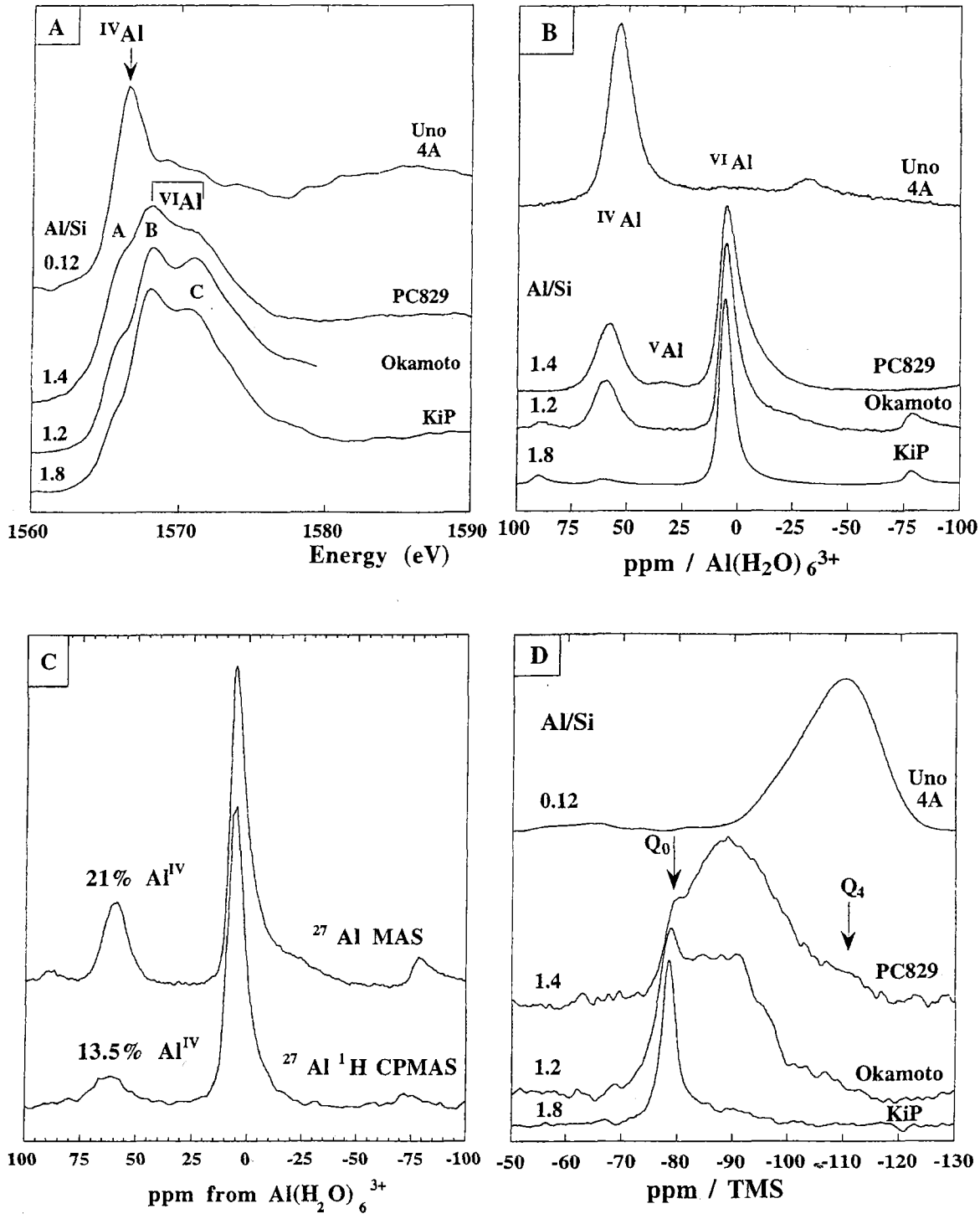

Figure 2: Al-K XANES (A), ^{27}Al MAS NMR (B), ^{27}Al ^{1}H CPMAS NMR (C), and ^{29}Si MAS NMR (D) data obtained on aluminosilicates

correspond to Si-O, and Si-(Si,Fe) shells (Manceau et al., 1995). Fourier filtered Si-(Si, Fe) contributions for Uno1 and nontronite are in phase over nearly the entire k range. This indicates that both materials have similar Si-Fe and Si-Si distances. Fitting resulted in 3 Si at 3.03 Å, and 1.5 Fe at 3.26 Å which is consistent with a phyllosilicate structure.

Si-bearing ferric oxides with lowest Fe/Si ratios have been only studied at Fe K-edge. In Fe K-edge XANES spectra, the low amplitude of the pre-edge feature together with the position of the main edge and its general shape evidenced that iron occurs as Fe^{3+} in

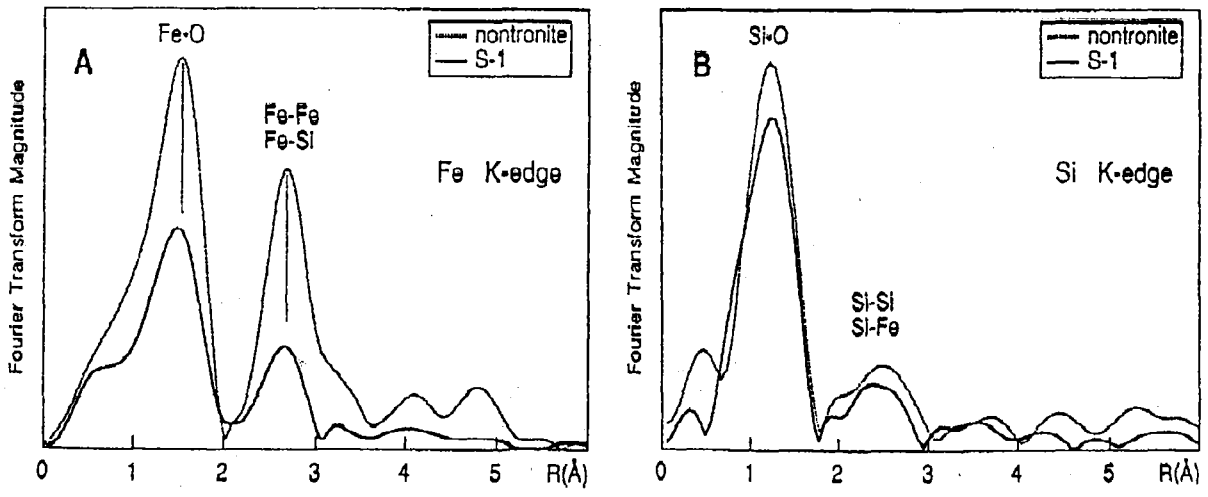

Figure 3: Fe-K and Si-K EXAFS data obtained on Uno1 iron silicate (from Manceau et al., 1995)
A: Comparison between Radial distribution functions of Uno1 and nontronite - Fe-K edge
B: Comparison between Radial distribution functions of Uno1 and nontronite - Si-K edge (S1 = Uno1)

octahedral coordination (Figure 4A). Nevertheless, the spectra of studied samples are different from those of all crystallized iron oxides. That evidenced that the local Fe environment is slightly different from that known in crystallized iron oxides. The first shell around Fe was fitted by considering 6 O atoms at 1.99 Å in agreement with Fe^{3+} in octahedral coordination. The RDF yields a second peak which is related to second neighbors around the Fe absorber (Figure 4B). That demonstrated that these poorly ordered mineral components are ordered at the local scale. This peak shows an assymetry towards high R values which is an indication of several subshells in this peak. The best fit was obtained by considering 2.9 Fe at 3.05 Å (edge-sharing octahedra), 1.7 Fe at 3.44 Å (double corner-sharing octahedra), and 0.45 Si at 3.29 Å (monodentate Si). These results evidenced the occurence of Si-O-Fe linkages in the structure of these natural iron oxides. The presence of Si in these iron oxides is responsible for their structural disorder and probably inhibits their crystal growth. It may be an important parameter for their higher stability in the environment than that of pure Fe end members (ferrihydrite s.s.).

CONCLUSIONS

With the examples considered in this paper, we demonstrated that natural gels are ordered at the atomic scale.

In allophanes, Al is distributed between octahedral and tetrahedral sites. The amount of ^{IV}Al increases as Al/Si ratio decreases, and in the studied opal ^{IV}Al is only present. ^{V}Al was also evidenced in Si-rich stream allophane. Besides, polymerization rate of silica units increases as Al/Si ratio decreases. In Si-rich allophanes, a large range of Si environment was found from Q^0 to Q^4 environments. Moreover, Si-rich allophanes have a local structure around Al and Si very diffrent of that known in kaolinite or halloysite.

Thus, tranformation of Si-rich allophanes to crystallized minerals implies dissolution-recrystallization processes (Ildefonse et al., 1995, Allard et al., 1997).

On the contrary, in iron silicate with Fe/Si=0.72, Si and Fe environments are close to those found in nontronite. The gel transformation to Fe-smectite may occur by long range ordering during ageing. Two-line Si-Fe oxides possess a local structure close to that found in goethite and akaganeite, and thus differ from that elucidated in pure Fe-end members. In ferrihydrite s.s., face-sharing octahedra have been evidenced (Combes et al., 1989, 1990). Ferric gels are constituted of a mixture of hematite nanocrystals and ferrihydrite (Manceau and Drits, 1993). In ferric silicate gels, the similarity of local structure around Fe in poorly ordered precursors and that known in crystallized minerals suggest a solid transformation during ageing. This difference between iron and aluminium is mainly due to the ability of Al to enter both tetrahedral and octahedral sites, while the affinity of iron for octahedral sites is higher at low temperature. Nevertheless, the systematic occurence of Si in natural Fe-oxides could promote their stability and hinder their transformation into crystalline minerals. This is important when considering their ability to sorb metals and to delay their migration in the environment.

The knowledge of the structure of gels makes it possible to investigate under which conditions these gels may last for geological periods and the parameters which allow us to consider them as natural analogues of the gels formed at the expense of the nuclear waste glasses.

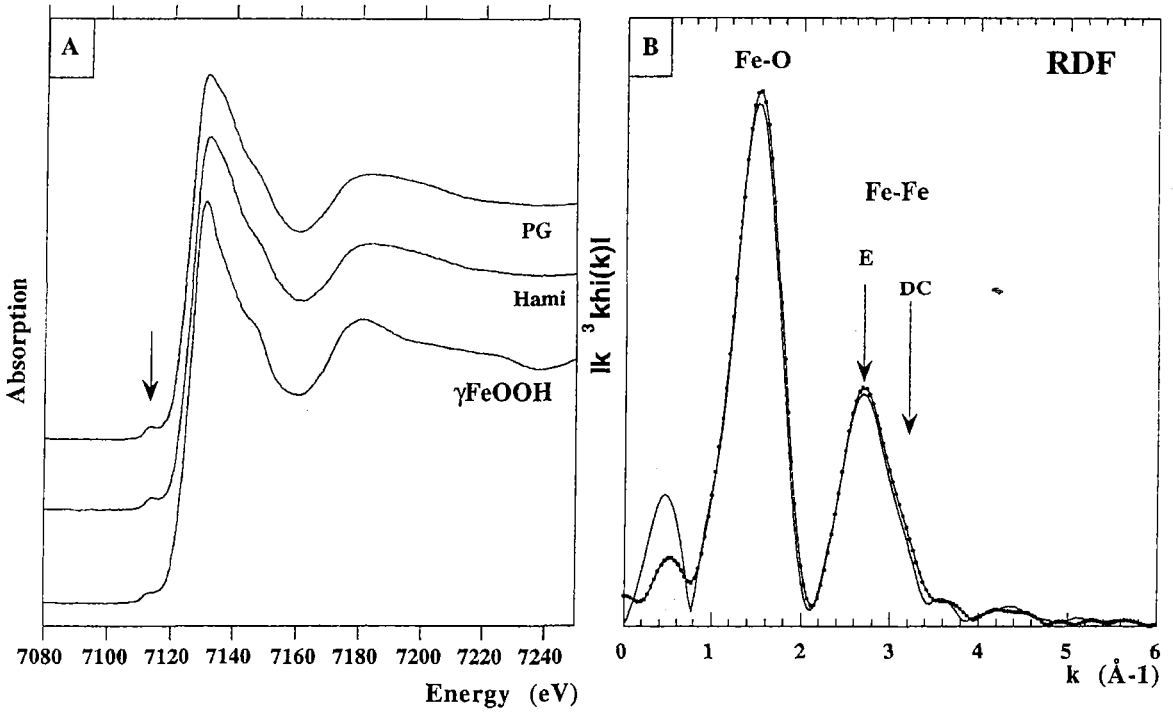

Figure 4: Fe-K edge spectroscopy of Si-bearing hydrated iron oxides
A: Fe-K Xanes, the arrow shows the low amplitude preedge feature characteristic of Fe^{3+} in octahedral coordination, see lepidocrocite γ-FeOOH spectrum for comparison;
B Radial distribution functions: two mains peaks may be observed and are related to first shell of (O, OH) and second shell of Fe atoms around absorbers (E: edge sharing octahedra, DC: double corner sharing octahedra); (dotted line: PG3, plain line:Hamilton

AKNOWLEDGEMENTS

This work is supported by CEA/DCC and ANDRA.

REFERENCES

Allard, Th., Calas, G., Ildefonse , Ph., Morin, G., et Muller, J.P. (1997) *C. R. Acad. Sci. Paris* (in press).

Childs, C.W., Parfitt, R.L. and Newman, R.H. (1990a) *Clay Minerals,* 25, 329-341.

Childs, C.W., Matsue, N., Yoshinaga, N. (1990b) *Clay Sci.*, 8, 9-15.

Combes, J.M., Manceau, A., Calas, G., and Bottero, J.Y. (1989) *Geochim. Cosmoch. Acta,* 53, 583-594.

Combes, J.M., Manceau, A., and Calas, G. (1990) *Geochim. Cosmoch. Acta,* 54, 1083-1091.

Farmer, V.C. and Russell, J.D. (1990) *Soil Colloids and Their Association in Aggregates,* M.F. De Boodt et al. (eds), Plenum Press, New-York, 165-178.

Ildefonse, Ph., Cabaret, D., Sainctavit, Ph., Calas, G., Flank, A.M., and Lagarde, P. (1997) *Physics and Chem. Miner.* (in press).

Ildefonse, Ph., Calas, G., Flank, A.M., and Lagarde, P. (1995) *Nuclear Instr. Methods in Phys. Res.*, B97, 172-175.

Ildefonse, Ph., Kirkpatrick, R.J., Montez, B., Calas, G., Flank, A.M., and Lagarde, P. (1994) *Clays and Clay Minerals,* 42, 276-287.

Inoue, K., and Yoshida, M. (1990) *Soil Sci. Plant. Nutr,* 36, 461-468.

Manceau, A., Ildefonse, Ph., Hazemann, J.L., Flank, A.M. and Gallup, D.L. (1995) *Clays and Clay Minerals,* 43, 304-317.

Manceau, A., and Drits, V. (1993) *Clay Minerals,* 28, 165-184.

Müller, D., Gessner, W., Behrens, H.J., Scheler, G. (1981) *Chem. Phys. Letters,* **79**, 59-62.

Van der Gaast, S.J., Wada, K., Wada, S.I., and Kakuto, Y. (1985) *Clays and Clay Minerals,* **33**, 237-243.

Wada, K. (1977) in *Minerals in Soil Environments,* J.B. Dixon and S.B. Weed,,eds., Soil Science Society America, Madison, Wisconsin, 603-638.

Yoshinaga, N. and Aomine, S. (1962) *Soil Sc. Plant. Nutr.*, **8**, 6-13.